Modeling ion channels from the cricket cercal sensory system

Carrie Diaz Eaton[*], Sharon Crook[*], Graham Cummins[**], Gwen Jacobs[**]

Department of Mathematics and Statistics, University of Maine, Orono, ME 04469

**Center for Computational Biology, Montana State University, Bozeman, MT 59715*

Abstract

We are interested in understanding how information about air current dynamics is represented and processed in the primary sensory interneurons of the cricket cercal system. In this work, we develop channel models based on voltage-clamp data from [9], use channel ensembles to construct model neurons, and analyze the underlying mathematical structure of these excitable systems. We also examine the behavior of the model neurons in response to constant frequency stimuli and its dependence on channel kinetics. This study provides a crucial step toward developing models for studying the contributions of channel dynamics to mechanisms underlying information processing in this system.

1. Introduction

The cercal system of the cricket gathers and processes information about the direction and dynamics of low-velocity air movements in the animal's immediate environment [10]. The receptor organs for this modality are the cerci, two appendages covered with

mechanoreceptor hairs that are sensitive to air current displacement. Afferent input is relayed to primary sensory interneurons in the terminal abdominal ganglion which project to higher centers of the nervous system [6]. We are interested in determining how information about the dynamics of air currents is represented and processed by these interneurons. Past modeling studies of primary sensory interneurons in the cricket, *Acheta domestica*, have used two ion channels, a transient sodium channel and delayed-rectifier type potassium channel, to model the spike-producing mechanism in these cells [2,3]. However, other ion channels are known to be present in the cells. Recent work by Kloppenburg and Hörner isolated and characterized four voltage-activated currents in two types of cultured primary sensory interneurons known as 8-1 (LGI) and 9-1 (MGI) in crickets *Gryllus bimaculatus* [9]. In this paper, we develop channel models based on this data, use ensembles of these channels to construct model neurons, and provide an analysis of the underlying mathematical structure of these excitable systems. This study provides a crucial step toward developing reduced models that can be used to study the contributions of channel dynamics to the biophysical mechanisms for information processing in this system.

2. Methods

We began by developing models for four different ion channels based on whole-cell patch-clamp data from cultured giant interneurons 8-1 and 9-1. The voltage-activated currents that were isolated and characterized in [9] are a transient K^+ current (I_K), a sustained K^+ A-current (I_A), a transient Na^+ current (I_{Na}), and a Ca^{2+} current (I_{Ca}). The mathematical expression for each model ionic current has the standard form

$I_c = \bar{g}_c y(v - v_c)$ where $\bar{g}_c$ is the maximal conductance, y is the gating variable for the activation of the current, v represents the membrane potential, and v_c is the reversal potential [4]. In some cases there is an additional gating variable that represents the gating of current inactivation. The kinetic equations for the gating variables have the form $\dot{y}(v) = (y_\infty(v) - y(v))/\tau_y(v)$ where $y_\infty(v)$ is the steady-state activation (or inactivation) curve, and $\tau_y(v)$ provides the time constant/voltage relationship for the activation (or inactivation) of the current. In this work, voltage-clamp data from [9] were used to determine the steady-state activation and inactivation curves for the gating variables for each channel type in the standard way [8]. The reversal potentials were also derived from experimental data [9]. In cases where the observed change in the gating variable is very fast, we replaced the gating variable with the steady-state curve in the channel model. A summary of all equations and parameters is provided in the Appendix.

Using the channel models for I_K, I_A, I_{Na}, and I_{Ca}, we created an initial model interneuron implemented as an active cable 1000 microns long and 5 microns in diameter with 200 compartments. This model allowed us to use parameter searching techniques to look for channel densities (maximal conductances) that would provide a parameter region corresponding to robust spiking. An additional goal was to find channel kinetics that would function well in both detailed biophysically-based models and reduced models. We also wanted to determine whether small variations in the channels developed using data from 8-1 and 9-1 could reproduce spike dynamics seen in other interneurons of interest such as 10-2 and 10-3. Parameter optimization was performed using a genetic algorithm. The fitness function was the root mean square error between a modeled action

potential waveform and a spike waveform recorded from the axon of a primary sensory interneuron. Additional error terms applied extra penalties associated with an unstable baseline potential, and the difference between modeled and actual spike height, spike width at half-maximum, and after-hyperpolarization depth and length.

After studying the effects of parameter changes, the resulting currents were used to create a reduced single-compartment interneuron model. This model was analyzed in order to determine the underlying mathematical structure of the channel dynamics. By adding an additional current we were also able to use the reduced model to examine the role of channel dynamics in determining cell response. The interneurons of interest exhibit a variety of responses for air-current stimuli including different levels of spike frequency adaptation. Previous experimental results have been used to classify interneurons as phasic (P-type), tonic (T-type) or a combination of phasic and tonic (PT-type) based on their adaptation rate in response to air-current stimuli with a sinusoidal velocity of fixed frequency [7]. P-type interneurons (e.g. 9-1) exhibit one to three spikes in response to a supra-threshold stimulus. T-type neurons (e.g. 10-2,10-3) respond in a tonic manner and synchronize with the alteration of the air current stimulus. A stronger stimulus intensity evokes doublet or triplet spikes during each cycle and a weaker stimulus intensity results in fewer spikes and weaker synchronization. In response to low intensity stimuli, PT-type neurons (e.g. 8-1, 9-2, 9-3) are phasic, but they exhibit a more tonic response when exposed to stronger stimuli. In order to replicate the observed results, we extended our model by including a Ca^{2+}-sensitive K^+ current, I_{AHP}. This current causes spike frequency

adaptation and is known to be present in these cells [1,9]. This approach also required an additional equation to model the changes in the concentration of Ca^{2+} in the cell.

3. Results

We found that model channels with kinetics based on [9] can be used to create robust spiking with waveforms that are similar to voltage traces obtained from the giant interneurons 8-1 and 9-1 for a wide range of parameters. However, we were unable to find parameters that created a good match for the spike shape typical of interneurons 10-3 and 10-2. The rise of the action potential was much too slow in our model even with the optimal parameter set. These results suggest that the channels underlying the spiking mechanism in 10-2 and 10-3 may be quite different from those found in the giant interneurons.

Mathematical analysis shows that our model is a type two model; that is, the transition to repetitive spiking as the applied current, I_{app}, increases occurs due to a Hopf bifurcation as described in Rinzel and Ermentrout [11]. Figure 1 shows a schematic of the bifurcation diagram for the model. For any particular vertical cross-section of the bifurcation diagram corresponding to a fixed value of I_{app}, the solid lines represent a stable steady-state or limit cycle and the dotted lines represent a similar unstable state for the system. One characteristic of type two neurons is the emergence of oscillations with nonzero frequency at the threshold required for spike initiation. This characteristic is consistent with experimental observations [7,9].

We are interested in studying the dynamics underlying the response properties of the three categories of interneurons (P, T and PT-types) when the air current velocity is sinusoidal with fixed frequency. In previous studies, we created models of afferent activity using a forward reconstruction based on electrophysiology data. These models show a sinusoidal change in average afferent activity for air-current stimuli with sinusoidal velocity. Because interneurons integrate excitatory inputs from hundreds of afferents, in this work we model the increase in afferent input for a sinusoidal air-current stimulus at an interneuron's preferred direction with a sinusoidal depolarizing current injection. By varying the amount of spike frequency adaptation and the dynamics of Ca^{2+} in our reduced models, we are able to replicate the behavior for all three cases. Figure 2 shows the model behavior for each type of interneuron in response to a weak and a strong sinusoidal depolarizing current injection.

In the future, further development of these reduced models will allow the study of mechanisms such as resonance [5], amplification of inputs, synaptic modulation due to depression and facilitation, and changes in channel kinetics due to neuromodulators with the goal of understanding the role of these mechanisms in neural encoding in this system.

Appendix

In the models, membrane potential is measured in mV, currents in $\mu A / cm^2$, time in ms, capacitance in $\mu F / cm^2$, and conductance in mS / cm^2.

Spiking Model

Current Balance Equation $\quad C_m \dfrac{dv}{dt} = I_{app} - I_A - I_K - I_{Na} - I_{Ca} - I_{lk}$

Ionic Currents and Kinetic Equations

$I_A = \bar{g}_A p_\infty^3 j(v - v_A)$

$p_\infty(v) = 1/(1 + e^{(v+27.4)/-17.4})$

$j_\infty(v) = 1/(1 + e^{(v+40.8)/12.3})$

$\tau_j(v) = 5 + c_j e^{(-.1v+2.99)}$

$I_K = \bar{g}_K n^3(v - v_K)$

$n_\infty(v) = 1/(1 + e^{(v+15.2)/-33.4})$

$\tau_n(v) = c_n e^{-.0254v}$

$I_{Na} = \bar{g}_{Na} m_\infty h(v - v_{Na})$

$m_\infty(v) = 1/(1 + e^{v/-8})$

$h_\infty(v) = 1/(1 + e^{(v+40.4)/8})$

$\tau_h(v) = c_h e^{-.0188v}$

$I_{Ca} = \bar{g}_{Ca} q_\infty f(v - v_{Ca})$

$q_\infty(v) = 1/(1 + e^{(v+25)/-2.5})$

$f_\infty(v) = 1/(1 + e^{(v+55)/9})$

$\tau_f(v) = c_f e^{-.0188v}$

Model Parameters

$v_K = -80$	$\bar{g}_K = 20$	$c_j = 1$	
$v_A = -80$	$\bar{g}_A = 5$	$c_n = 7.03$	
$v_{Ca} = 50$	$\bar{g}_{Ca} = 1$	$c_h = .6632$	$C_m = 1$
$v_{Na} = 68$	$\bar{g}_{Na} = 50$	$c_f = 1$	
$v_{lk} = -60$	$\bar{g}_{lk} = .1$		

Adapting Model

Current Balance Equation and Calcium Equation

$C_m \dfrac{dv}{dt} = I_{app} - I_A - I_K - I_{Na} - I_{Ca} - I_{AHP} - I_{lk}$

$\dfrac{d[Ca]}{dt} = -\alpha I_{Ca} - \beta[Ca]$

Ionic currents and kinetic equations are the same as above except

$I_{AHP} = \bar{g}_{AHP} r(v - v_K)$

$r_\infty(v) = .0005[Ca]$

$\tau_r(v) = 1/(\min(.00001[Ca], .01) + .001)$

Other parameters are the same as above except

P-type Model: $\bar{g}_{AHP} = 15$, $\alpha = -20$, $\beta = -.005$, $c_j = 1$, $c_n = 2$, $c_h = .6$, $c_f = 10$

T-type Model: $\bar{g}_{AHP} = 3$, $\alpha = -5$, $\beta = -.01$, $c_j = 1$, $c_n = 3.5$, $c_h = 1$, $c_f = 10$

PT-type Model: $\bar{g}_{AHP} = 10$, $\alpha = -10$, $\beta = -.005$, $c_j = 1$, $c_n = 2$, $c_h = .6$, $c_f = 10$

References

[1]   H. Clague, F. Theunnissen and J.P. Miller, Effects of adaptation on neural coding by primary sensory interneurons in the cricket cercal system, J. Neurophysiol. 77 (1997) 207-220.

[2]   S. Crook, J. Miller and G. Jacobs, Modeling frequency encoding in the cricket cercal sensory system, Neurocomp. 44 (2002) 769-773.

[3]   G.I. Cummins, S.M. Crook, A.G. Dimitrov, T. Ganje, G.A. Jacobs and J.P. Miller, Structural and biophysical mechanisms underlying dynamic sensitivity of primary sensory interneurons in the cricket cercal sensory system, Neurocomp. (2003)

[4]   A.L. Hodgkin and A.F. Huxley, A quantitative description of membrane current and its application to conduction and excitation in nerve, J. Physiol. 117 (1952) 500-544.

[5]   B. Hutcheon and Y. Yarom, Resonance, oscillation and the intrinsic frequency preferences of neurons, Trends Neurosci. 23 (2000) 216-222.

[6]   G.A. Jacobs and R.K. Murphey, Segmental origins of the cricket giant interneuron system, J. Comp. Neurol. 265 (1987) 145-157.

[7]   M. Kanou and T. Shimozawa, A threshold analysis of cricket cercal interneurons by an alternating air-current stimulus, J. Comp. Physiol. A 154 (1984) 357-365.

[8]   J. Keener and J. Sneyd, Mathematical Physiology (Springer, New York, 1998).

[9]   P. Kloppenburg and M. Hörner, Voltage-activated currents in identified giant interneurons isolated from adult crickets Gryllus bimaculatus, J. Exp. Biology. 201 (1998) 2529-2541.

[10] J.P. Miller, F.E. Theunissen and G.A. Jacobs, Representation of sensory information in the cricket cercal sensory system. I. Response properties of the primary interneurons, J. Neurophys. 66 (1991) 1680-1689.

[11]   J. Rinzel and B. Ermentrout, Analysis of neural excitability and oscillation, in: C. Koch and I. Segev, eds., Methods in Neuronal Modeling, (MIT Press, Cambridge, Massachusetts, 1998) 251-291.

Figures

Figure 1. Schematic of the bifurcation diagram for the model as the level of injected current, I_{app}, varies. Note that the model exhibits a Hopf bifurcation at the transition to repetitive firing.

Figure 2. Model interneuron responses for injected depolarizing sinusoidal current. Parameters for each model are provided in the Appendix. Panels A and B demonstrate results for P-type model interneurons in response to low and high levels of injected current respectively. Panels C and D demonstrate responses for T-type model interneurons for low and high levels of injected current respectively, and Panels E and F demonstrate responses for PT-type model interneurons. In each case, the injected current has the form $I_{app} = a\sin(2t\pi\varpi) + a$ where a determines the amplitude and ϖ determines the frequency. For low intensity stimuli, $a = 10$, and for high intensity stimuli, $a = 50$.
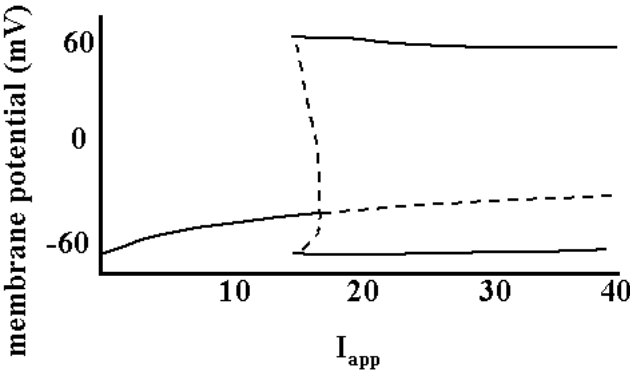
Figure 1

Figure 2